

Rashba spin torque in ferromagnetic metal films

Xuhui Wang,* Christian Ortiz Pauyac, and Aurelien Manchon
King Abdullah University of Science and Technology (KAUST),
Physical Science and Engineering Division, Thuwal 23955-6900, Saudi Arabia
(Dated: June 29, 2012)

In a two-dimensional ferromagnetic metal film lacking inversion symmetry, the itinerant electrons mediate the interaction between the Rashba spin-orbit interaction and the ferromagnetic order parameter, leading to a Rashba spin torque exerted on the magnetization. Using Keldysh technique, in the presence of both magnetism and spin-orbit coupling, we derive a spin diffusion equation that provides a coherent description to the diffusive spin dynamics. The characteristics of the spin torque and its implication on magnetization dynamics are discussed for a wide range of relative strength between Rashba spin-orbit coupling and the ferromagnetic exchange.

PACS numbers: 75.60.Jk

I. INTRODUCTION

By transferring angular momentum between electronic spin and orbital degrees of freedom, spin-orbit coupling fills the need for electrical manipulation of spins. Outstanding examples are the electrically generated bulk spin polarization^{1,2} and the well-known spin-Hall effect (SHE)³⁻⁵ in a two dimensional electron gas where the spin-orbit interaction, particularly of the Rashba-type,⁶ plays the leading role. Rashba spin-orbit interaction not only introduces an effective field perpendicular to the linear momentum but also provides the backbone to the spin relaxation through the so-called D'yakonov-Perel mechanism,⁷ which is dominant in a two-dimensional system. Besides its prominent role in semiconductors, Rashba spin-orbit coupling is believed to exist at ferromagnetic/heavy metal and ferromagnetic/metal-oxide interfaces, where the inversion symmetry breaking offers a potential gradient empowering the spin-orbit coupling.

Meanwhile, magnetism continuously stimulates the industrial and academic appetite. In the pursuit of fast magnetization switching, Slonczewski-Berger spin transfer torque⁸ employs a polarized spin current instead of a cumbersome magnetic field. This celebrated scheme demands noncollinear magnetic textures in forms of, for example, spin valves or domain wall structures.⁹

In the presence of inversion symmetry breaking (such as asymmetric interfaces), a ferromagnetic metal layer assembles both magnetism and spin-orbit coupling, offering an alternative switching mechanism:¹⁰⁻¹² spin-orbit coupling transfers the orbital angular momentum carried by an electric current to the electronic spin, thus creating an effective magnetic field (Rashba field). As long as the effective field is misaligned with the magnetization direction, the so-called Rashba torque emerges to excite the magnetization.

Current-driven magnetization dynamics by spin-orbit torque has been demonstrated by several experiments in metal oxide based systems.¹³⁻¹⁵ In fact, the Rashba torque can be categorized into a broader family of spin-orbit interaction-induced torques that has been observed in diluted magnetic semiconductors.¹⁶⁻¹⁸ Re-

cently, Miron *et al.*,¹⁹ has demonstrated the current-induced magnetization switching using a *single* ferromagnet in Pt/Co/AlO_x trilayers, which further consolidates the feasibility of Rashba torque. The same type of torque is predicted to improve current-driven domain wall motion,^{11,20} which is also supported by experimental observations.²¹ At this stage, we are mindful of an alternative explanation based on the spin-Hall effect occurring in the underlying heavy metal layer (such as Pt or Ta).²² An in-depth discussion on the distinction between the spin-Hall effect induced torque (called SHE torque thereafter) and the Rashba one is offered elsewhere.²³

In searching for a general form of the Rashba torque in an ultrathin ferromagnetic metal film, we found an expression that consists of two components:¹² an in-plane torque (aligned along the direction $\mathbf{m} \times (\hat{\mathbf{y}} \times \mathbf{m})$) and an out-of-plane one (aligned to $\hat{\mathbf{y}} \times \mathbf{m}$), given $\hat{\mathbf{y}}$ is the in-plane direction transverse to the current transport direction and \mathbf{m} is the orientation of magnetization. In the case of a weak Rashba spin-orbit coupling, numerical solutions on a two-dimensional nanowire with one open transport direction has been carried out to appreciate the significance of diffusive motion on the spin torque. We found that the magnitude of the in-plane Rashba torque is enhanced by narrowing the magnetic wire.¹²

In this article, we give a full theoretical derivation of the coupled diffusive equation for spin dynamics in a ferromagnetic metal film and describe the general form of the Rashba torque from weak to strong Rashba coupling limits. In Sec. II, we combine the Keldysh formalism and the gradient expansion technique to derive a diffusion equation for charge and nonequilibrium spin densities. To demonstrate that the diffusion equation provides a coherent framework to describe the spin dynamics, we dedicate Sec. III to the spin diffusion in a ferromagnetic metal, which shows an excellent agreement to early result on the same system. In Sec. IV, we illustrate that the absence of magnetism (in our diffusion equation) describes the well-known phenomenon of electrically induced spin polarization. The cases of a weak and a strong spin-orbit coupling are discussed in Sec. V and Sec. VI, respectively, where we provide an analytical form of the Rashba torque

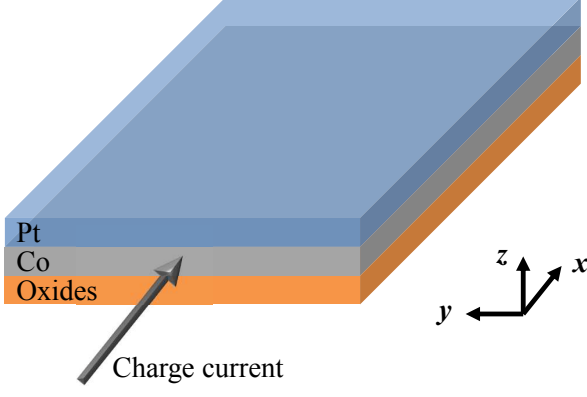


FIG. 1. (color online). A ferromagnetic thin film (such as Co) is sandwiched between a heavy metal layer (such as Pt) and an oxide (such as AlO_x). A charge current is flowing in the ferromagnetic film along the \hat{x} direction.

in an infinite medium. Section VII is dedicated to, for a wide range of relative strength between Rashba coupling and the exchange splitting, numerical solutions of the diffusion equation. In Sec. VIII, we discuss the implication of the Rashba torque on magnetization dynamics.

II. DIFFUSION EQUATIONS

As depicted in Fig.1, the system of interest is defined as a quasi-two-dimensional ferromagnetic metal layer rolled out in the $x - y$ plane. Two asymmetric interfaces provide a confinement in the z direction, along which the potential gradient generates a Rashba spin-orbit coupling. Therefore a single particle Hamiltonian for an electron of momentum $\hat{\mathbf{k}}$ is ($\hbar = 1$ is assumed throughout)

$$\hat{H} = \frac{\hat{\mathbf{k}}^2}{2m} + \alpha \hat{\boldsymbol{\sigma}} \cdot (\hat{\mathbf{k}} \times \hat{\mathbf{z}}) + \frac{1}{2} \Delta_{xc} \hat{\boldsymbol{\sigma}} \cdot \mathbf{m} + \hat{H}^i \quad (1)$$

where $\hat{\boldsymbol{\sigma}}$ is the Pauli matrix, m the effective mass, and \mathbf{m} the magnetization direction. The ferromagnetic exchange splitting is given by Δ_{xc} and α represents the Rashba constant (parameter). The Hamiltonian $\hat{H}^i = \sum_{j=1}^N V(\mathbf{r} - \mathbf{r}_j)$ sums the contribution of the non-magnetic impurity scattering potential $V(\mathbf{r})$ localized at \mathbf{r}_j .

To derive a diffusion equation for the nonequilibrium charge and spin densities, we employ the Keldysh formalism.²⁴ Using the Dyson equation, in a 2×2 spin space, we obtain a kinetic equation that assembles the retarded (advanced) Green's function \hat{G}^R (\hat{G}^A), the Keldysh component of the Green function \hat{G}^K , and the self-energy $\hat{\Sigma}^K$, i.e.,

$$[\hat{G}^R]^{-1} \hat{G}^K - \hat{G}^K [\hat{G}^A]^{-1} = \hat{\Sigma}^K \hat{G}^A - \hat{G}^R \hat{\Sigma}^K, \quad (2)$$

where all Green's functions are full functions with interactions taken care of by the self-energies $\hat{\Sigma}^{R,A,K}$. The retarded (advanced) Green's function in momentum and energy space is

$$\hat{G}^{R(A)}(\mathbf{k}, \epsilon) = \frac{1}{\epsilon - \epsilon_{\mathbf{k}} - \hat{\boldsymbol{\sigma}} \cdot \mathbf{b}(\mathbf{k}) - \hat{\Sigma}^{R(A)}(\mathbf{k}, \epsilon)}, \quad (3)$$

where $\epsilon_{\mathbf{k}} = \mathbf{k}^2/(2m)$ is the single particle energy. We have introduced a \mathbf{k} -dependent total effective field $\mathbf{b}(\mathbf{k}) = \Delta_{xc} \mathbf{m}/2 + \alpha(\mathbf{k} \times \mathbf{z})$ of the magnitude $b_k = |\Delta_{xc} \mathbf{m}/2 + \alpha(\mathbf{k} \times \mathbf{z})|$ and the direction $\hat{\mathbf{b}} = \mathbf{b}(\mathbf{k})/b_k$.

Neglecting localization effects and electron-electron interactions, we assume a short-range δ -function type impurity scattering potential. At a low impurity concentration and a weak coupling to electrons, a second-order Born approximation is justified,²⁴ i.e., the self-energy due to impurity scattering is²⁵

$$\hat{\Sigma}^{R,A,K}(\mathbf{r}, \mathbf{r}') = \frac{\delta(\mathbf{r}, \mathbf{r}')}{m\tau} \hat{G}^{R,A,K}(\mathbf{r}, \mathbf{r}), \quad (4)$$

where the momentum relaxation time reads

$$\frac{1}{\tau} \approx 2\pi \int \frac{d^2 \mathbf{k}'}{(2\pi)^2} |V(\mathbf{k} - \mathbf{k}')|^2 \delta(\epsilon_{\mathbf{k}} - \epsilon_{\mathbf{k}'}). \quad (5)$$

$V(\mathbf{k})$ is the Fourier transform of the scattering potential and the magnitude of \mathbf{k} and \mathbf{k}' is evaluated at Fermi vector k_F .

The quasiclassical distribution function $\hat{g} \equiv \hat{g}_{\mathbf{k},\epsilon}(T, \mathbf{R})$, defined as the Wigner transform of the Keldysh function $\hat{G}^K(\mathbf{r}, t; \mathbf{r}', t')$, is obtained by integrating out the relative spatial-temporal coordinates while retaining the center-of-mass ones $\mathbf{R} = (\mathbf{r} + \mathbf{r}')/2$ and $T = (t + t')/2$. As the spatial profile of the quasiclassical distribution function is smooth at the scale of Fermi wavelength, we may apply the gradient expansion technique on Eq.(2),²⁶ which gives us a transport equation associated with macroscopic quantities. Under the gradient expansion, the left hand side of Eq.(2) becomes

$$\begin{aligned} & [\hat{G}^R]^{-1} \hat{G}^K - \hat{G}^K [\hat{G}^A]^{-1} \\ & \approx [\hat{g}, \hat{\boldsymbol{\sigma}} \cdot \mathbf{b}(\mathbf{k})] + \frac{i}{\tau} \hat{g} + i \frac{\partial \hat{g}}{\partial T} \\ & \quad + \frac{i}{2} \left\{ \frac{\mathbf{k}}{m} + \alpha(\hat{\mathbf{z}} \times \hat{\boldsymbol{\sigma}}), \nabla_{\mathbf{R}} \hat{g} \right\}, \end{aligned} \quad (6)$$

where $\{\cdot, \cdot\}$ is the anticommutator. The relaxation time approximation indulges the right hand side of Eq.(2) as

$$\begin{aligned} & \hat{\Sigma}^K \hat{G}^A - \hat{G}^R \hat{\Sigma}^K \\ & \approx \frac{1}{\tau} \left[\hat{\rho}(\epsilon, T, \mathbf{R}) \hat{G}^A(\mathbf{k}, \epsilon) - \hat{G}^R(\mathbf{k}, \epsilon) \hat{\rho}(\epsilon, T, \mathbf{R}) \right] \end{aligned} \quad (7)$$

where we have introduced the density matrix by integrating out \mathbf{k}' in \hat{g} , i.e.,

$$\hat{\rho}(E, T, \mathbf{R}) = \frac{1}{2\pi N_0} \int \frac{d^2 \mathbf{k}'}{(2\pi)^2} \hat{g}_{\mathbf{k}',\epsilon}(T, \mathbf{R}). \quad (8)$$

For the convenience of discussion, the time variable is changed from T to t . At this stage, we have a kinetic equation depending on $\hat{\rho}$ and \hat{g}

$$\begin{aligned} i[\hat{\sigma} \cdot \mathbf{b}(\mathbf{k}), \hat{g}] + \frac{1}{\tau} \hat{g} + \frac{\partial \hat{g}}{\partial t} + \frac{1}{2} \left\{ \frac{\mathbf{k}}{m} + \alpha(\hat{\mathbf{z}} \times \hat{\sigma}), \nabla_{\mathbf{R}} \hat{g} \right\} \\ = \frac{i}{\tau} \left[\hat{G}^R(\mathbf{k}, \epsilon) \hat{\rho}(\epsilon) - \hat{\rho}(\epsilon) \hat{G}^A(\mathbf{k}, \epsilon) \right]. \end{aligned} \quad (9)$$

A Fourier transformation on temporal variable to the frequency domain ω leads to

$$\Omega \hat{g} - b_k[\hat{U}_k, \hat{g}] = i\hat{K}, \quad (10)$$

where $\Omega = \omega + i/\tau$ and the operator $\hat{U}_k \equiv \hat{\sigma} \cdot \hat{\mathbf{b}}$ satisfies $\hat{U}_k \hat{U}_k = 1$. The right hand side of Eq.(10) is partitioned according to

$$\begin{aligned} \hat{K} = & \underbrace{-\frac{1}{2} \left\{ \frac{\mathbf{k}}{m} + \alpha(\hat{\mathbf{z}} \times \hat{\sigma}), \nabla_{\mathbf{R}} \hat{g} \right\}}_{\hat{K}^{(1)}} \\ & + \underbrace{\frac{i}{\tau} \left[\hat{G}^R(\mathbf{k}, \epsilon) \hat{\rho}(\epsilon) - \hat{\rho}(\epsilon) \hat{G}^A(\mathbf{k}, \epsilon) \right]}_{\hat{K}^{(0)}}. \end{aligned} \quad (11)$$

The equilibrium part is denoted by $\hat{K}^{(0)}$ and the gradient term $\hat{K}^{(1)}$ is treated as perturbation. Functions \hat{g} and $\hat{\rho}$ are both in frequency domain.

We solve Eq. (10) formally to find a solution to \hat{g}

$$\hat{g} = i \frac{(2b_k^2 - \Omega^2) \hat{K} + 2b_k^2 \hat{U}_k \hat{K} \hat{U}_k - \Omega b_k [\hat{U}_k, \hat{K}]}{\Omega(4b_k^2 - \Omega^2)} \equiv \mathcal{L}[\hat{K}]. \quad (12)$$

An iteration procedure to solve Eq.(12) has been outlined in Ref.[25]. We adopt the procedures here: according to the partition scheme of \hat{K} , we use $\hat{K}^{(0)}$ to obtain the zeroth order approximation given by $\hat{g}^{(0)} \equiv \mathcal{L}[\hat{K}^{(0)}(\hat{\rho})]$ which replaces \hat{g} in $\hat{K}^{(1)}$ to generate a correction due to the gradient term, i.e., $\hat{K}^{(1)}(\hat{g}^{(0)})$; we further insert $\hat{K}^{(1)}(\hat{g}^{(0)})$ back to Eq.(12) to obtain a correction $\mathcal{L}[\hat{K}^{(1)}(\hat{g}^{(0)})]$, then we have the first order approximation to the quasiclassical distribution function,

$$\hat{g}^{(1)} = \hat{g}^{(0)} + \mathcal{L}[\hat{K}^{(1)}(\hat{g}^{(0)})]. \quad (13)$$

The above procedure is repeated to desired orders using

$$\hat{g}^{(n)} = \hat{g}^{(n-1)} + \mathcal{L}[\hat{K}^{(1)}(\hat{g}^{(n-1)})]. \quad (14)$$

In this paper, the second order approximation is sufficient. The full expression of the second order approximation for \hat{g} is tedious thus to be excluded in the following. The diffusion equation is derived by an angle averaging in momentum space, which allows all terms that are of odd order in k_i ($i = x, y$) to vanish while the combinations such as $k_i k_j$ contribute to the averaging by a factor $k_F^2 \delta_{ij}$.²⁶

Furthermore, a Fourier transform from frequency domain back to the real time brings a diffusion-like equation for the density matrix,

$$\begin{aligned} \frac{\partial}{\partial t} \hat{\rho}(t) = & D \nabla^2 \hat{\rho} - \frac{1}{\tau_{xc}} \hat{\rho} + \frac{1}{2\tau_{xc}} (\hat{\mathbf{z}} \times \hat{\sigma}) \cdot \hat{\rho} (\hat{\mathbf{z}} \times \hat{\sigma}) + iC [\hat{\mathbf{z}} \times \hat{\sigma}, \nabla \hat{\rho}] - B \{ \hat{\mathbf{z}} \times \hat{\sigma}, \nabla \hat{\rho} \} \\ & + \Gamma [(\mathbf{m} \times \nabla)_z \hat{\rho} - \hat{\sigma} \cdot \mathbf{m} \nabla \hat{\rho} \cdot (\hat{\mathbf{z}} \times \hat{\sigma}) - (\hat{\mathbf{z}} \times \hat{\sigma}) \cdot \nabla \hat{\rho} \hat{\sigma} \cdot \mathbf{m}] \\ & + \frac{1}{2T_{xc}} (\hat{\sigma} \cdot \mathbf{m} \hat{\rho} \hat{\sigma} \cdot \mathbf{m} - \hat{\rho}) - i\tilde{\Delta}_{xc} [\hat{\sigma} \cdot \mathbf{m}, \hat{\rho}] - 2R \{ \hat{\sigma} \cdot \mathbf{m}, (\mathbf{m} \times \nabla)_z \hat{\rho} \}, \end{aligned} \quad (15)$$

where all quantities are evaluated at Fermi energy ϵ_F . In a two-dimensional system, the diffusion constant $D = \tau v_F^2/2$ is given in terms of Fermi velocity v_F and momentum relaxation time τ . The renormalized exchange splitting reads $\tilde{\Delta}_{xc} = (\Delta_{xc}/2)/(4\xi^2 + 1)$ where $\xi^2 =$

$(\Delta_{xc}^2/4 + \alpha^2 k_F^2) \tau^2$. The other parameters are given by

$$\begin{aligned} C &= \frac{\alpha k_F v_F \tau}{(4\xi^2 + 1)^2}, \quad \Gamma = \frac{\alpha \Delta_{xc} v_F k_F \tau^2}{2(4\xi^2 + 1)^2}, \\ R &= \frac{\alpha \Delta_{xc}^2 \tau^2}{2(4\xi^2 + 1)}, \quad B = \frac{2\alpha^3 k_F^2 \tau^2}{4\xi^2 + 1}, \\ \frac{1}{\tau_{xc}} &= \frac{2\alpha^2 k_F^2 \tau}{4\xi^2 + 1}, \quad \frac{1}{T_{xc}} = \frac{\Delta_{xc}^2 \tau}{4\xi^2 + 1}. \end{aligned}$$

τ_{xc} is the relaxation time due to the D'yakonov-Perel mechanism.¹ Equation (15) is valid in the dirty limit $\xi \ll 1$, which enables the approximation $1 + 4\xi^2 \approx 1$. Charge density n and the nonequilibrium spin density \mathbf{S}

are introduced by the vector decomposition of the density matrix $\hat{\rho} = n/2 + \mathbf{S} \cdot \hat{\boldsymbol{\sigma}}$. In real experiments,^{13,19,21} spin transport in a ferromagnetic film suffers from random magnetic scatterers, for which we introduce, phenomenologically, an isotropic spin-flip relaxation \mathbf{S}/τ_{sf} .

Eventually, we obtain a set of diffusion equations for the charge and spin densities, i.e.,

$$\frac{\partial n}{\partial t} = D\nabla^2 n + B\nabla_z \cdot \mathbf{S} + \Gamma\nabla_z \cdot \mathbf{m}n + R\nabla_z \cdot \mathbf{m}(\mathbf{S} \cdot \mathbf{m}), \quad (16)$$

and

$$\begin{aligned} \frac{\partial \mathbf{S}}{\partial t} = & D\nabla^2 \mathbf{S} - \frac{\mathbf{S}_{\parallel}}{\tau_{\parallel}} - \frac{\mathbf{S}_{\perp}}{\tau_{\perp}} - \Delta_{xc} \mathbf{S} \times \mathbf{m} - \frac{\mathbf{m} \times (\mathbf{S} \times \mathbf{m})}{T_{xc}} \\ & + B\nabla_z n + 2C\nabla_z \times \mathbf{S} + 2R(\mathbf{m} \cdot \nabla_z n)\mathbf{m} \\ & + \Gamma[\mathbf{m} \times (\nabla_z \times \mathbf{S}) + \nabla_z \times (\mathbf{m} \times \mathbf{S})], \end{aligned} \quad (17)$$

where $\nabla_z \equiv \hat{z} \times \nabla$. The spin density $\mathbf{S}_{\parallel} \equiv S_x \hat{x} + S_y \hat{y}$ is relaxed at a rate $1/\tau_{\parallel} \equiv 1/\tau_{xc} + 1/\tau_{sf}$ while $\mathbf{S}_{\perp} \equiv S_z \hat{z}$ has a rate $1/\tau_{\perp} \equiv 2/\tau_{xc} + 1/\tau_{sf}$.

For a broad range of the relative strength between the spin-orbit coupling and the exchange splitting, i.e., $\alpha k_F/\Delta_{xc}$, Eq.(16) and Eq.(17) describe the spin dynamics in a ferromagnetic film. When the magnetism vanishes ($\Delta_{xc} = 0$), the B term provides a source that generates spin density electrically.^{2,25} On the other hand, when the Rashba spin-orbit coupling is absent ($\alpha = 0$), the first two lines in Eq.(17) describe a diffusive motion of spin density in a ferromagnetic metal, which, to be shown in the next section, agrees excellently with early results.²⁷ The C term describes the coherent precession of the spin density around the effective Rashba field. The precession of the spin density (induced by the Rashba field) around the exchange field is described by the Γ term, is thus at a higher order (compared to C) in the dirty limit for $\Gamma = \Delta_{xc}\tau C/2$. The R term contributes to the magnetization renormalization.

III. SPIN DIFFUSION IN A FERROMAGNET

Spin diffusion in a ferromagnet has been discussed actively in the field of spintronics.^{27–30} In this section we show explicitly that, by suppressing the Rashba spin-orbit coupling, Eq.(17) is able to describe spin diffusion in a ferromagnetic metal.

A vanishing Rashba spin-orbit coupling means $\alpha = 0$, Eq.(17) reduces to

$$\frac{\partial \mathbf{S}}{\partial t} = D\nabla^2 \mathbf{S} + \frac{\mathbf{m} \times \mathbf{S}}{\tau_{\Delta}} - \frac{\mathbf{S}}{\tau_{sf}} - \frac{\mathbf{m} \times (\mathbf{S} \times \mathbf{m})}{T_{xc}}, \quad (18)$$

where $\tau_{\Delta} \equiv 1/\Delta_{xc}$ sets the time scale for the coherent precession of the spin density around the magnetization. This equation only differs from the result of Ref.[28] by a dephasing term of the transverse component of the spin density that is of the time scale T_{xc} .

In a ferromagnetic metal, we may divide the spin density into a *longitudinal* component that follows the magnetization direction adiabatically, and a deviation that is *perpendicular* to the magnetization, i.e., $\mathbf{S} = s_0 \mathbf{m} + \delta \mathbf{S}$ where s_0 is the local equilibrium spin density. Such a partition, after restoring the electric field by $\nabla \rightarrow \nabla + e\mathbf{E}\partial_e$, gives rise to

$$\begin{aligned} \frac{\partial}{\partial t} \delta \mathbf{S} + \frac{\partial}{\partial t} s_0 \mathbf{m} \\ = s_0 D\nabla^2 \mathbf{m} + D\nabla^2 \delta \mathbf{S} + DeP_F \mathcal{N}_F \mathbf{E} \cdot \nabla \mathbf{m} \\ - \frac{\delta \mathbf{S}}{\tau_{sf}} - \frac{s_0 \mathbf{m}}{\tau_{sf}} - \frac{\delta \mathbf{S}}{T_{xc}} + \Delta_{xc} \mathbf{m} \times \delta \mathbf{S}, \end{aligned} \quad (19)$$

where the magnetic order parameter is allowed to be spatial dependent $\mathbf{m} = \mathbf{m}(\mathbf{r}, t)$. The energy derivative is treated as $\partial_e \mathbf{S} \approx P_F \mathcal{N}_F \mathbf{m}$ given P_F the spin polarization and \mathcal{N}_F the density of state, both are at Fermi energy ϵ_F .

In a smooth magnetic texture, the characteristic length scale of the magnetic profile is much larger than the length scale for electron transport, we discard the contribution $D\nabla^2 \delta \mathbf{S}$.²⁷ The diffusion of the equilibrium spin density follows $s_0 D\nabla^2 \mathbf{m} \approx s_0 \mathbf{m}/\tau_{sf}$. In this paper, we retain only terms that are at first order in temporal derivative, which simplifies Eq.(19) to

$$\varsigma \frac{\delta \mathbf{S}}{\tau_{\Delta}} - \frac{\mathbf{m} \times \delta \mathbf{S}}{\tau_{\Delta}} = DeP_F \mathcal{N}_F \mathbf{E} \cdot \nabla \mathbf{m} - s_0 \frac{\partial \mathbf{m}}{\partial t}. \quad (20)$$

The last equation can be solved exactly

$$\begin{aligned} \delta \mathbf{S} = \frac{\tau_{\Delta}}{1 + \varsigma^2} \left[\frac{P_F}{e} \mathbf{m} \times (\mathbf{j}_e \cdot \nabla) \mathbf{m} + \varsigma \frac{P_F}{e} (\mathbf{j}_e \cdot \nabla) \mathbf{m} \right. \\ \left. - s_0 \mathbf{m} \times \frac{\partial \mathbf{m}}{\partial t} - \varsigma s_0 \frac{\partial \mathbf{m}}{\partial t} \right] \end{aligned} \quad (21)$$

where $\varsigma = \tau_{\Delta}(1/\tau_{sf} + 1/T_{xc})$ and the electric current $\mathbf{j}_e = e^2 n \tau \mathbf{E}/m$ is given in terms of electron density n . Apart from the transverse dephasing time implemented in parameter ς , the nonequilibrium spin density Eq.(21) agrees excellently with Eq.(8) in Ref.[27].

Given the knowledge of the nonequilibrium spin density, the spin torque, defined as

$$\mathbf{T} = -\frac{1}{\tau_{\Delta}} \mathbf{m} \times \delta \mathbf{S} + \frac{1}{T_{xc}} \delta \mathbf{S}, \quad (22)$$

is given by

$$\begin{aligned} \mathbf{T} = \frac{1}{1 + \varsigma^2} \left[-\eta s_0 \frac{\partial \mathbf{m}}{\partial t} + \beta s_0 \mathbf{m} \times \frac{\partial \mathbf{m}}{\partial t} \right. \\ \left. + \eta \frac{P_F}{e} (\mathbf{j}_e \cdot \nabla) \mathbf{m} - \beta \frac{P_F}{e} \mathbf{m} \times (\mathbf{j}_e \cdot \nabla) \mathbf{m} \right] \end{aligned} \quad (23)$$

where $\eta = 1 + \varsigma \tau_{\Delta}/T_{xc}$ and $\beta = \tau_{\Delta}/\tau_{sf}$. Assuming a long dephasing time of the transverse component (i.e., $T_{xc} \rightarrow \infty$), then $\eta \approx 1$ and Eq. (23) reproduces the Eq.(9) in Ref.[27]. On the other hand, a short spin dephasing time (i.e., $T_{xc} \rightarrow 0$) yields $\eta/(1 + \varsigma^2) \rightarrow 1$ and $\beta/(1 + \varsigma^2) \rightarrow 0$ which results in a pure adiabatic torque, i.e., the torque reduces to the first and third terms in Eq.(23).

IV. ELECTRICALLY GENERATED SPIN DENSITY

The effect of an electrically generated nonequilibrium spin density due to spin-orbit coupling² can be extracted from Eq.(17) by setting exchange interaction zero (i.e., $\Delta_{xc} = 0$). Retaining D'yakonov-Perel as the only spin relaxation mechanism and letting $\tau_{sf} = \infty$, Eq.(17) reads

$$D\nabla^2 \mathbf{S} - \frac{\mathbf{S} + S_z \hat{\mathbf{z}}}{\tau_{xc}} + 2C\nabla_z \times \mathbf{S} + B\nabla_z n = 0 \quad (24)$$

which reduces to describe the well-known spin-Hall effect.^{25,31,32} Besides the spin relaxation [the second term in Eq. (24)], the spin dynamics is controlled by two competing effects: the spin precession around Rashba field (third term) and the electrical spin generation first pointed out by Edelstein.² In the case of an infinite medium along transport direction, i.e., the $\hat{\mathbf{x}}$ direction, Eq.(24) leads to a solution

$$\mathbf{S} = eE\tau_{xc}B\frac{n}{\epsilon_F}\hat{\mathbf{y}} = \frac{eE\zeta}{\pi v_F}\hat{\mathbf{y}}, \quad (25)$$

where only the linear term in electric field has been retained. On the right hand side, we have used the charge density in a 2D system $n = k_F^2/(2\pi)$ and introduced the parameter $\zeta = \alpha k_F \tau$ as used in Ref.[25].

It is worth pointing out that in the case of a weak spin-orbit coupling, only the spin precession term survives, whereas in the case of strong coupling, the electrical spin generation dominates. As will be exposed in the remaining of this work, this distinction defines two regimes where the spin torque symmetry and efficiency are different.

V. WEAK SPIN-ORBIT COUPLING

A weak Rashba spin-orbit coupling implies a low D'yakonov-Perel relaxation rate $1/\tau_{xc} \propto \alpha^2$, such that $\tau_{xc} \gg \tau_{sf}, \tau_\Delta$, which allows spin relaxation to be dominated by random magnetic impurities. In this regime, when comparing the contribution due to C and Γ term to that from B and R , the later are at a higher order in α , thus to be disregarded. As mentioned in the previous section, this is a regime when spin precession about the Rashba field dominates the electrical spin generation.

We consider a stationary state meaning $\partial \mathbf{S}/\partial t = 0$. An electric field is applied along the $\hat{\mathbf{x}}$ direction $\mathbf{E} = E\hat{\mathbf{x}}$. In an infinite medium,¹⁰ all the spatial derivatives vanishes ($\nabla \rightarrow 0$) and the dynamic equation reads

$$\begin{aligned} & 2eEC\hat{\mathbf{y}} \times \partial_\epsilon \mathbf{S} + eE\Gamma [\hat{\mathbf{y}} \times (\mathbf{m} \times \partial_\epsilon \mathbf{S}) + \mathbf{m} \times (\hat{\mathbf{y}} \times \partial_\epsilon \mathbf{S})] \\ &= -\frac{\mathbf{m} \times \mathbf{S}}{\tau_\Delta} + \frac{\mathbf{m} \times (\mathbf{S} \times \mathbf{m})}{T_\perp} + \frac{\mathbf{S}}{\tau_{sf}} \end{aligned} \quad (26)$$

In addition to spin density induced by the exchange splitting, a weak spin-orbit interaction contributes to a deviation (in spin density) that can be considered as perturbation. Therefore, we may divide $\mathbf{S} = \mathbf{S}_\perp + \mathbf{S}_\parallel \mathbf{m}$ into a longitudinal and a transverse component. Equation (26) reduces to

$$\begin{aligned} & \frac{1}{\tau_\Delta} \mathbf{m} \times \mathbf{S}_\perp - \frac{1}{T_\perp} \mathbf{S}_\perp - \frac{1}{\tau_{sf}} S_\parallel \mathbf{m} \\ &= -eEP_F \mathcal{N}_F [2C\hat{\mathbf{y}} \times \mathbf{m} + \Gamma \mathbf{m} \times (\hat{\mathbf{y}} \times \mathbf{m})], \end{aligned} \quad (27)$$

where $1/T_\perp \equiv 1/T_{xc} + 1/\tau_{sf}$ and we have again employed the approximation $\partial_\epsilon \mathbf{S} \approx P_F \mathcal{N}_F \mathbf{m}$ and replaced the energy derivative of the charge density by the density of states at Fermi energy, i.e., $\partial_\epsilon n \approx n/\epsilon_F = \mathcal{N}_F$. We solve Eq.(27) to obtain a nonequilibrium spin density

$$\begin{aligned} \mathbf{S}_\perp &= \frac{\tau_\Delta}{1 + \zeta^2} eEP_F \mathcal{N}_F [(2C + \zeta\Gamma) \mathbf{m} \times (\hat{\mathbf{y}} \times \mathbf{m}) \\ &\quad - (\Gamma - 2\zeta C)(\hat{\mathbf{y}} \times \mathbf{m})]. \end{aligned} \quad (28)$$

and $\mathbf{S}_\parallel = 0$. In Eq.(28), the second component, oriented along the direction $\hat{\mathbf{y}} \times \mathbf{m}$, is actually perpendicular to the plane spanned by the magnetization \mathbf{m} and the effective Rashba field that is along $\hat{\mathbf{y}}$. This field, as to be shown below, contributes to a torque that fulfils the symmetry described in recent experiments.¹⁹

The definition Eq.(22) leads to a general expression for the Rashba torque

$$\mathbf{T} = T_\perp \hat{\mathbf{y}} \times \mathbf{m} + T_\parallel \mathbf{m} \times (\hat{\mathbf{y}} \times \mathbf{m}), \quad (29)$$

which consists of both *out-of-plane* and *in-plane* components with magnitudes determined by

$$T_\perp = \frac{eEP_F \mathcal{N}_F}{1 + \zeta^2} (2\eta C + \beta\Gamma), \quad (30)$$

$$T_\parallel = \frac{eEP_F \mathcal{N}_F}{1 + \zeta^2} (\eta\Gamma - 2\beta C). \quad (31)$$

Note that the sign of the in-plane torque, Eq. (31), can change depending on the competition between spin relaxation and precession.

To compare directly with the results in Ref.[10], we allow the spin relaxation time $\tau_{sf} \rightarrow \infty$, then $\beta \approx 0$. We also consider the transverse dephasing time to be negligible ($T_{xc} \rightarrow 0$). Under these assumptions, $\eta/(1 + \zeta^2) \approx 1$ and we have $T_\perp \approx 2eEP_F \mathcal{N}_F C$ and $T_\parallel \approx eEP_F \mathcal{N}_F \Gamma$. In the dirty limit, $\Gamma \ll C$ due to $\Delta_{xc}\tau \ll 1$. By making use of the relation for the polarization $P_F = \Delta_{xc}/\epsilon_F$ and the Drude relation $j_e = e^2 n \tau E/m$, we obtain the out-of-plane torque

$$\mathbf{T} = 2 \frac{\alpha m \Delta_{xc}}{e \epsilon_F} j_e \hat{\mathbf{y}} \times \mathbf{m}, \quad (32)$$

which agrees excellently with the spin torque in an infinite system in the corresponding limit as derived in Ref.[10].

VI. STRONG SPIN-ORBIT COUPLING

The opposite limit to Sec.V is a strong spin-orbit coupling. In this case, we consider that $\alpha k_F \gg \Delta_{xc}$ and the D'yakonov-Perel relaxation mechanism is dominating, i.e., $1/\tau_{xc} \gg 1/\tau_{sf}$, since $1/\tau_{xc} \propto \alpha^2$. The spin precession about Rashba field becomes negligible compared to the electrical spin generation ($C \ll B$) and therefore, it is not physical to simply assume that the direction of spin density is dominantly aligned along the magnetization direction, as what is treated in the case of a weak spin-orbit coupling. For the nonequilibrium spin density, a self-consistent solution from Eq.(17) is more justified.

As in Sec.V, we consider an infinite system where an electric field \mathbf{E} is applied along the \hat{x} direction, while the magnetization direction is left arbitrary. We approximate the energy derivative by $\partial_\epsilon \approx 1/\epsilon_F$. The above assumptions simplify Eq.(17) to

$$\frac{\mathbf{S} \times \mathbf{m}}{\tau_\Delta} + \frac{\mathbf{m} \times (\mathbf{S} \times \mathbf{m})}{T_{xc}} - \frac{2eEC}{\epsilon_F} \hat{y} \times \mathbf{S} + \frac{(\mathbf{S} + S_z \hat{z})}{\tau_{xc}} = \frac{eEn}{\epsilon_F} B \hat{y}, \quad (33)$$

where a strong spin-orbit coupling renders Γ and R terms negligible. By considering $T_{xc} \gg \tau_\Delta, \tau_{xc}$, Eq. (33) reduces to

$$\frac{\mathbf{S} \times \mathbf{m}}{\tau_\Delta} + \frac{(\mathbf{S} + S_z \hat{z})}{\tau_{xc}} - \frac{2eEC}{\epsilon_F} \hat{y} \times \mathbf{S} = \frac{eEn}{\epsilon_F} B \hat{y}, \quad (34)$$

which is a set of linear equations for the nonequilibrium spin density. We are interested in the linear response regime, which implies that at the distance as defined by the Fermi wave length $1/k_F$, we have $eE/k_F \ll \alpha k_F$. Therefore, up to the first order in exchange splitting, we extract the spin density from the above equation

$$\mathbf{S} = eE\tau_{xc}B \frac{n}{\epsilon_F} \left(\hat{y} - \chi \hat{y} \times \mathbf{m} - \frac{\chi}{2} m_x \hat{z} \right) \quad (35)$$

where $\chi \equiv \tau_{xc}/\tau_\Delta$ and we have used the identity $\hat{y} \times \mathbf{m} = m_z \hat{x} - m_x \hat{z}$. It is interesting to point out that, when taking the limit $\Delta_{xc} \rightarrow 0$ hence $\chi \rightarrow 0$, Eq.(35) precisely reduces to the spin density that is generated entirely due to spin-orbit interaction, i.e., Eq.(25).

The spin density Eq.(35) yields a spin torque

$$\mathbf{T} = \frac{\alpha m \Delta_{xc}}{e\epsilon_F} j_e (\hat{y} \times \mathbf{m} + \chi \mathbf{m} \times (\hat{y} \times \mathbf{m}) - \frac{\chi}{2} m_x \hat{z} \times \mathbf{m}). \quad (36)$$

This torque is different from the weak Rashba limit and has a strong implication in terms of magnetization dynamics. When the magnetization is aligned perpendicular to the film plane $\mathbf{m} = \hat{z}$,¹⁹

$$\mathbf{T}_{(\mathbf{m}=\hat{z})} = \frac{\alpha m \Delta_{xc}}{e\epsilon_F} j_e (\hat{y} \times \hat{z} + \chi \hat{z} \times (\hat{y} \times \hat{z})), \quad (37)$$

where the *in-plane* torque (second term) can be understood as either being generated from an effective field along the \hat{x} direction or from a spin current that is polarized along the \hat{y} direction. In the strong spin-orbit limit, simply increasing the magnitude of Rashba coupling is not the most optimal way to enhance the *in-plane* torque efficiency since the D'yakonov-Perel spin relaxation rate increases as α^2 . The implication of this torque on the current-driven magnetization dynamics is discussed in Sec.VIII.

In this paper, our numerical results as presented in the following section is based on the setup where $\mathbf{m} = \hat{x}$. The torque then reads

$$\mathbf{T}_{(\mathbf{m}=\hat{x})} = \frac{\alpha m \Delta_{xc}}{e\epsilon_F} j_e \left(\hat{y} \times \hat{x} + \frac{\chi}{2} \hat{x} \times (\hat{y} \times \hat{x}) \right). \quad (38)$$

For the same parameters, an in-plane magnetization produces an in-plane torque with a magnitude that is only half of the one with an out-of-plane magnetization, see Eq.(37).

VII. NUMERICAL RESULTS

We numerically solve the Eqs.(16) and (17) to demonstrate that they provide a coherent framework to describe the spin dynamics in the diffusive regime for a wide range of parameters. Here, we consider an in-plane magnetization that lies along the \hat{x} direction and we refer the readers to Ref.[12] for another case where the magnetization is perpendicular to the thin film plane. Using the finite element method, for a two-dimensional electron system we adopt the following boundary conditions: (i) vanishing spin accumulation at the edges along the transverse direction i.e., $\mathcal{S}(y=0, L) = 0$; (ii) an electric field is implemented along the \hat{x} direction therefore we set the charge densities at two ends of the propagation direction to be constant $n_L = n_R = n_F$. The first boundary condition implies a strong spin-flip scattering at the edges, which is consistent with the experimental observations in spin-Hall effect.⁵ The second boundary condition sets the charge density at the Fermi level. Equivalently, one can apply a voltage drop along the transport direction instead of an explicit inclusion of an electric field.

The numerical results of nonequilibrium spin densities are summarized in Fig.2. When viewing from the top panels (a,b) to the lower ones (c,d), for a fixed value of the exchange splitting, the system transits from the weak spin-orbit coupling regime to the strong spin-orbit coupling regime. As an illustration of this transition, the S_z component of the spin accumulation evolves from a symmetric spatial distribution in the weak spin-orbit coupling regime [$\alpha = 0.0005$ eV nm in Fig. 1(a)] to an antisymmetric spatial distribution along y in the strong coupling regime [$\alpha = 0.05$ eV nm in Fig. 1(c)]. Note that throughout this transition, the in-plane spin density S_y is robustly constant in the bulk of the wire.

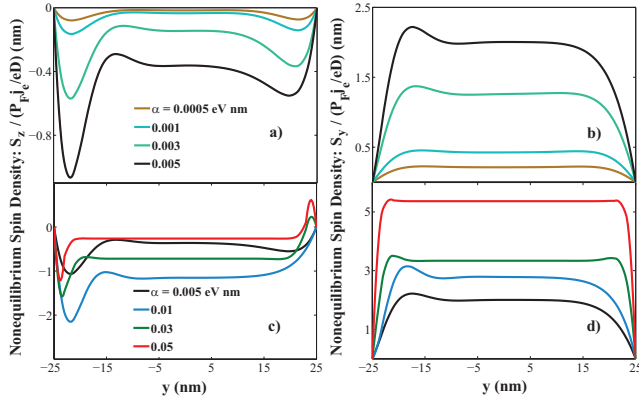


FIG. 2. (color online). Spatial profile of the nonequilibrium spin density S_z (a),(c) and S_y (b),(d) for various values of the Rashba constant. The width of the wire is $L = 50$ nm. The magnetization direction is along the \hat{x} axis. Other parameters are: momentum relaxation time $\tau = 10^{-15}$ s, exchange splitting $\Delta_{xc} = 0.01$ eV, spin relaxation time $\tau_{sf} = 10^{-12}$ s, and the Fermi vector $k_F = 4.3$ nm $^{-1}$.

This symmetry transition and the emergence of peaks close to the boundaries are a manifestation of the competition of the Rashba and exchange fields. In the weak coupling regime, the total field is dominated by the exchange field pointing at the \hat{x} direction, around which the spin accumulation profile that is spatially symmetric. As the spin-orbit coupling increases, the total field is tilted towards the \hat{y} axis, then the spin projections along $+y$ and $-y$ are no longer symmetric, as indicated by curves with intermediate α values in Fig.2(a)(b). In the strong coupling regime, when Rashba coupling is larger than the exchange field, the antisymmetric profile in S_z and the symmetric one of S_y follow naturally from the spin-Hall effect induced by the Rashba spin-orbit interaction.

The out-of-plane and in-plane torques are plotted in Fig.3 with respect to the Rashba constant α for various exchange splitting. The transition regions are of particular interest. During the transition from the weak to strong coupling, the magnitude of the out-of-plane torque T_{\perp} (see Fig.3(a)) first reaches a plateau, then rises again as the α increases. In the large α limit, though the magnitude of the torque increases with α , the torque efficiency defined as $dT_{\perp}/d\alpha$ is actually smaller than it is in the weak coupling. This picture is consistent with a semi-classical Boltzmann equation description employed in Ref. [10]. This behavior is due to the different processes generating the Rashba torque in both regimes. As discussed in Sec. V and VI, in the weak coupling regime, the torque is dominated by the spin precession around the Rashba field; whereas in the strong coupling, the electrical generation of the spin density dominates. These two distinct processes have different efficiencies.

The in-plane torque T_{\parallel} behaves differently. In the strong coupling limit, T_{\parallel} is proportional to $1/\alpha$ due to the large D'yakonov-Perel spin relaxation rate that is of the order α^2 . Therefore a stronger spin-orbit coupling means

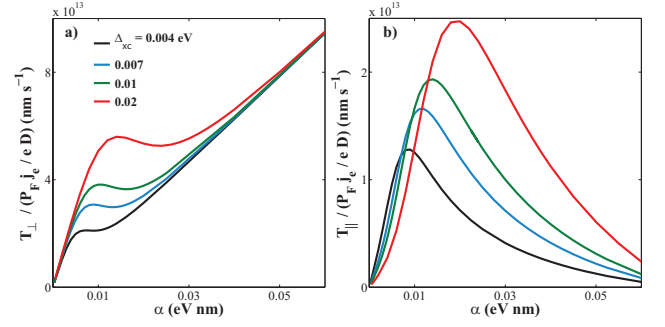


FIG. 3. (color online). The magnitude of the out-of-plane torque T_{\perp} (a) and in-plane torque T_{\parallel} (b) as a function of Rashba constant for various exchange splitting. Other parameters are the same as in Fig.2.

a decrease in the torque magnitude. In fact, the transition suggests that the optimal magnitude of the in-plane torque is achieved when the exchange energy is about the same order of magnitude of the Rashba splitting αk_F .

VIII. DISCUSSION

Current-induced magnetization dynamics in a single ferromagnetic layer has been observed in various structures that involve interfaces between transition metal ferromagnets, heavy metals and/or metal-oxide insulators. Existing experimental systems are Pt/Co/AlO $_x$,^{13,14,19,21} Ta/CoFeB/MgO,¹⁵ Pt/NiFe and Pt/Co bilayers.²² Besides the structural complexity in such systems, an unclear picture of spin-orbit coupling in the bulk and at the interfaces places a challenge to understand the nature of the torque.

A. Validity of Rashba model

The celebrated Rashba-type effective interfacial spin-orbit Hamiltonian was pioneered by E. I. Rashba to model the influence of asymmetric interfaces in semiconducting two-dimensional electron gas:⁶ a sharp potential drop, emerging at the interface (say, in the $x - y$ plane) between two materials, gives rise to a potential gradient ∇V that is normal to the interface, i.e., $\nabla V \approx \xi(\mathbf{r})\hat{z}$. In case a rotational symmetry exists in-plane, a spherical Fermi surface assumption allows the spin-orbit interaction Hamiltonian to have the form $\hat{H}_R = \alpha \hat{\sigma} \cdot (\mathbf{p} \times \hat{z})$, where $\alpha \approx \langle \xi \rangle / 4m^2c^2$. As a matter of fact, in semiconducting interfaces where the transport is described by a limited number of bands around a high symmetry point, the Rashba form can be recovered by $\mathbf{k} \cdot \mathbf{p}$ theory.³³

As far as metallic interfaces are concerned, a spin-orbit splitting of the Rashba-type in the conduction band has been observed at Au surfaces,³⁴ Gd/GdO interfaces,³⁵ Bi surfaces and compounds,³⁶ and metallic quantum wells.³⁷ The presence of a Rashba interaction at oxide hetero-

interfaces³⁸ has also been reported recently. It is worth noticing that the symmetry breaking-induced spin splitting of the conduction band seems rather general and might not be restricted to heavy metal interfaces.³⁷

In transition metals, however, the free electron approximation fails to accurately characterize the band structure due to both a large number of band crossing at the Fermi energy and a strong hybridization among s , p and d orbitals. Density functional theory (DFT) is successful in investigating spin-orbit interaction at metallic surfaces.^{39,40} For example, in Refs.[40], the authors observe a band splitting that possesses similar properties as Rashba spin-orbit interaction and decays exponentially away from the surface.⁴⁰ Alternatively, the spin-orbit interaction at metallic surfaces has been addressed using tight-binding models for the p orbitals.^{41,42} At such sharp interfaces, the magnitude of the orbital angular momentum (OAM) is considered to play a dominant role at the onset of a Rashba-type spin splitting.

This finding is consistent with the long standing work on interfacial magnetic anisotropy at a ferromagnet/heavy metal⁴³ and ferromagnetic/metal-oxide interfaces,⁴⁴ where a perpendicular magnetic anisotropy arises from the orbital overlap between the $3d$ states of the ferromagnets and the spin-orbit coupled states of the normal metal. The observation of perpendicular magnetic anisotropy at Co/metal-oxide interfaces tends to support the major role of large interfacial OAM in the onset of interfacial spin-orbit effects.^{42,44}

The presence of interfacial Rashba spin-orbit coupling has also been shown to explain tunneling anisotropic magnetoresistance⁴⁵ and interfacial perpendicular magnetic anisotropy.⁴⁶ Assuming a simplistic free electron dispersion, these models properly capture the symmetries of the observed effects, demonstrating the seminal role of interfacial Rashba spin-orbit coupling in these systems.

All the previous theoretical and experimental studies strongly suggest that the interfacial spin splitting exists in the presence of a large OAM and potential gradient. However, a microscopic description of realistic interfaces is absent. Although the Rashba spin-orbit interaction is a convenient Hamiltonian to extract qualitative behaviors, its applicability to realistic metallic interfaces with complex band structures remains to be tested. Meanwhile, a recently proposed phenomenon called spin-orbit sound may provide an alternative experimental tool to determine the strength of the coupling.⁴⁷

B. Comparison between SHE torque and Rashba torque

At this stage, it is interesting to compare the parameter dependence of the in-plane torque T_{\parallel} (in Eq.(31)) and the torque generated by a spin-Hall effect⁴⁸ in the bulk of a heavy metal material such as Pt. In the later case, the torque $\mathbf{T}^{(\text{SH})}$ exerted on the normal metal/ferromagnet interface is obtained by projecting out the spin current

($\mathbf{j}^{(\text{SH})}$ due to spin-Hall effect) that is transverse to the magnetization direction.²² In the bulk, the spin current can be estimated using the ratio between spin-Hall (σ^{SH}) and longitudinal (σ_{xx}) conductivities (the so-called spin-Hall angle), i.e.,

$$\mathbf{j}^{(\text{SH})} = \frac{\sigma^{SH}}{\sigma_{xx}} \mathbf{j}_e. \quad (39)$$

A perturbation calculation using the second-order Born approximation gives rise to a spin current thus the torque with a magnitude given by,

$$T^{(\text{SH})} = \frac{\eta_{so} m \gamma}{2e\tau_{\text{tr}}^0} j_e \quad (40)$$

where, in general, $\gamma > 1$ is a dimensionless parameter taking into account both side-jump ($\gamma = 1$) and skew-scattering ($\gamma > 1$) contributions to the spin-Hall effect.⁴⁹ η_{so} is the spin-orbit coupling parameter and τ_{tr}^0 is the transport relaxation time due to bulk impurities, the same definitions as in Ref.[49] except here the definition of spin current differs by a unit $1/(2e)$. Meanwhile, the magnitude of the in-plane torque Eq. (31) can be simplified to, since $\Delta_{xc}\tau \ll 1$

$$T_{\parallel} \approx \frac{4\alpha m}{\epsilon_F e \tau_{sf}} j_e. \quad (41)$$

The spin-orbit coupling parameter α in our definition in Eq.(1) has the unit of energy. Equations (41) and (40) actually show that the in-plane Rashba torque and the spin-Hall torque have a very similar parameter dependence.

Using a diffusive description of the bilayer system consisting of ferromagnet/heavy metal, it was shown that both SHE torque and Rashba torque adopt a similar form,

$$\mathbf{T} = T_{\parallel} \mathbf{m} \times (\hat{\mathbf{y}} \times \mathbf{m}) + T_{\perp} \hat{\mathbf{y}} \times \mathbf{m}. \quad (42)$$

The similarity in the geometrical form of the two torques imply that, in principle, they are able to induce the same type of magnetic excitation.²³

C. Magnetization Dynamics

In Pt/Co/AlO_x trilayers, Miron *et al* have observed a current-driven domain wall nucleation,¹³ an enhanced current-driven domain wall velocity²¹ and a magnetization switching.¹⁹ The symmetry of the spin torque needed to explain the experimental findings agree well with Rashba torque proposed in Ref. [10 and 12]. In a similar structure, Pi *et al*¹⁴ and Suzuki *et al*¹⁵ also observed an effective fieldlike torque to be interpreted by the Rashba torque.

1. Magnetization switching

Our previous discussions suggest that both Rashba torque and SHE torque possess a general form²³

$$\mathbf{T} = T_{\perp} \hat{\mathbf{y}} \times \mathbf{m} + T_{\parallel} \mathbf{m} \times (\hat{\mathbf{y}} \times \mathbf{m}) \quad (43)$$

that consists of a fieldlike torque (T_{\perp}) and an (anti-)damping term (T_{\parallel}). As a consequence, both Rashba torque and SHE torque have the appropriate symmetry to excite the magnetization of a single ferromagnet and induce switching, as observed by Miron *et al.*¹⁹ and Liu *et al.*²² In the case of a large Rashba spin-orbit coupling, the torque acquires an additional component that acts like an effective magnetic field along the $\hat{\mathbf{z}}$ direction, vanishing as the magnetization component m_x is zero (see Section VI), which provides an additional torque that helps destabilize the magnetization.

2. Current-driven domain wall motion

The influence of Rashba/SHE torque on a domain wall can be illustrated within the rigid Bloch wall approximation. The perpendicularly magnetized Bloch wall is parameterized by $\mathbf{m} = (\cos \phi \sin \theta, \sin \phi \sin \theta, \cos \theta)$ where $\phi = \phi(t)$ and $\theta(x, t) = 2 \tan^{-1}[e^{(x-x_c(t))/\Delta}]$, where x_c refers to the center of the domain wall and Δ is defined as the domain wall width. To describe the dynamics of a Bloch wall, Landau-Lifshitz-Gilbert (LLG) equation

$$\partial_t \mathbf{m} = -\gamma \mathbf{m} \times \mathbf{H}_{eff} + \alpha_G \partial_t \mathbf{m} \times \mathbf{m} + \boldsymbol{\tau} \quad (44)$$

has to be augmented by the current induced torque $\boldsymbol{\tau}$

$$\begin{aligned} \boldsymbol{\tau} = & b_J (\mathbf{u} \cdot \nabla) \mathbf{m} - \beta b_J \mathbf{m} \times (\mathbf{u} \cdot \nabla) \mathbf{m} \\ & + b_J (\tau_{\perp} \hat{\mathbf{y}} \times \mathbf{m} + \tau_{\parallel} \mathbf{m} \times (\hat{\mathbf{y}} \times \mathbf{m}) \\ & + \tau_z m_x \hat{\mathbf{z}} \times \mathbf{m}). \end{aligned} \quad (45)$$

The torque $\boldsymbol{\tau}$ is written in the most general form, where the first two terms are the regular adiabatic and the so-called non-adiabatic torques; the next two terms (τ_{\parallel} and τ_{\perp}) emerge from the presence of Rashba and/or spin Hall effect and the last term τ_z appears only in large Rashba limit (see Sec. VI). The magnitude of the adiabatic torque is $b_J = \mu_B P j_e / e$. The effective field is given by

$$\mathbf{H}_{eff} = \frac{2A}{M_s} \nabla^2 \mathbf{m} + H_K m_x \hat{\mathbf{x}} + H_{\perp} m_z \hat{\mathbf{z}}. \quad (46)$$

Parameter γ in LLG is the gyromagnetic ratio, α_G is the Gilbert damping, A is the exchange constant, M_s is the saturation magnetization, H_K is the in-plane magnetic anisotropy and H_{\perp} is the combination of an out-of-plane anisotropy and a demagnetizing field. The magnetization dynamics can be obtained readily from Eqs. (44)-(46) by

integrating over the magnetic volume

$$\partial_t \phi + \alpha_G \frac{\partial_t x_c}{\Delta} = \left[\frac{\Delta \pi}{2} (\tau_{\parallel} - \frac{\tau_z}{2}) \cos \phi - \beta \right] \frac{b_J}{\Delta} \quad (47)$$

$$\alpha_G \partial_t \phi - \frac{\partial_t x_c}{\Delta} = -\gamma \frac{H_K}{2} \sin 2\phi + \left(1 + \frac{\Delta \pi}{2} \tau_{\perp} \cos \phi \right) \frac{b_J}{\Delta}. \quad (48)$$

We observe that the in-plane torque τ_{\parallel} distorts the domain wall texture, while the perpendicular torque τ_{\perp} drives the domain wall motion. The additional torque τ_z , arising in the large Rashba limit, only contributes to the in-plane torque. Therefore, in the following, we will refer to the in-plane torque as $\tau_{\parallel}^* = \tau_{\parallel} - \tau_z/2$. Below the Walker breakdown ($\partial_t \phi = 0$), the velocity is given by

$$\begin{aligned} \partial_t x_c = & - \left(\beta - \frac{\Delta \pi}{2} \tau_{\parallel}^* \cos \phi \right) \frac{b_J}{\alpha_G} \\ \gamma \frac{H_K}{2} \sin 2\phi = & \left[\alpha_G - \beta + \frac{\Delta \pi}{2} (\alpha_G \tau_{\perp} + \tau_{\parallel}^*) \cos \phi \right] \frac{b_J}{\alpha_G \Delta}, \end{aligned} \quad (49)$$

where the tilting angle ϕ is given by the competition between the magnetic anisotropy, the non-adiabatic torque, and the Rashba/SHE torque. In the case of weak Rashba ($\tau_z = 0$), assuming $\tau_{\parallel} = \beta \tau_{\perp}$ and omitting the correction to the spin precession, we recover the results of Ref. [52]. When neglecting the in-plane torque and accounting for the perpendicular Rashba torque ($\tau_{\parallel}^* = 0$), the Rashba torque only acts like an effective transverse field and enhances the Walker breakdown limit²¹ [see Eq. (50)].

Accounting for the in-plane component τ_{\parallel} arising either from corrections to Rashba torque or from the SHE, this torque appears to modify the domain wall velocity. Therefore, depending on the strength and the sign of Rashba/SHE torque as well as on the resulting tilting angle ϕ , it is possible to obtain a vanishing or even a reversed domain wall velocity, as has been shown numerically in Ref. [52] and illustrated in Eq. (49). A full scale numerical investigation is beyond the scope of this article, but it will help understand the profound effect of Rashba and SHE torque on the domain wall structures.

IX. CONCLUSION

Using Keldysh technique, in the presence of both magnetism and a Rashba spin-orbit coupling, we derive a spin diffusion equation that provides a coherent description to the diffusive spin dynamics. In particular, we have derived a general expression for the Rashba torque in the bulk of a ferromagnetic metal layer, at both weak and strong Rashba limits. We find that the torque is in general composed of two components, a field-like torque and an (anti-)damping one. Being aware of the recent alternative interpretation on the current-induced magnetization switching in a single ferromagnet, we have discussed the difference between the Rashba and the SHE torques.

While exploring the common features, we found that the magnetization dynamics driven by the Rashba torque presents several interesting similarities to that induced by SHE torque. Nevertheless, further investigation involving structural modification of the system is expected to provide a deeper knowledge on the nature of the interfacial spin-orbit interaction as well as the current-induced

magnetization switching in a single ferromagnet.

ACKNOWLEDGMENTS

We thank G. E. W. Bauer, J. Sinova, M. D. Stiles, X. Waintal, and S. Zhang for stimulating discussions. We are specially grateful to K. -J. Lee and H. -W. Lee for inspiring discussion about the magnetization dynamics.

-
- * xuhui.wang@kaust.edu.sa
- ¹ M. I. D'yakonov and V. I. Perel, Sov. Phys. JETP Lett. **13**, 467 (1971).
 - ² V. M. Edelstein, Solid State Commun. **73**, 233 (1990).
 - ³ S. Murakami, N. Nagaosa, and S.-C. Zhang, Science **301**, 1348 (2003).
 - ⁴ J. Sinova *et al.*, Phys. Rev. Lett. **92**, 126603 (2004).
 - ⁵ Y. K. Kato, R. C. Myers, A. C. Gossard, and D. D. Awschalom, Science **306**, 1910 (2004).
 - ⁶ Yu. A. Bychkov and E. I. Rashba, J. Phys. C: Solid State Phys. **17**, 6039 (1984).
 - ⁷ M. I. D'yakonov and V. I. Perel, Sov. Phys. Solid State **13**, 3023 (1971).
 - ⁸ J. C. Slonczewski, J. Magn. Magn. Mater. **159**, L1 (1996); L. Berger, Phys. Rev. B **54**, 9353 (1996).
 - ⁹ M. D. Stiles and J. Miltat, Top. Appl. Phys. **101**, 225 (2006); D. C. Ralph and M. D. Stiles, J. Magn. Magn. Mater. **320**, 1190 (2008); J. Z. Sun and D. C. Ralph, J. Magn. Magn. Mater. **320**, 1227 (2008).
 - ¹⁰ A. Manchon and S. Zhang, Phys. Rev. B **78**, 212405 (2008); Phys. Rev. B **79**, 094422 (2009).
 - ¹¹ A. Matos-Abiad and R. L. Rodriguez-Suarez, Phys. Rev. B **80**, 094424 (2009); I. Garate and A. H. MacDonald, Phys. Rev. B **80**, 134403 (2009); P. M. Haney, and M. D. Stiles, Phys. Rev. Lett. **105**, 126602 (2010).
 - ¹² X. Wang and A. Manchon, Phys. Rev. Lett. **108**, 117201 (2012). In Fig.3(a) of this paper, a typo misplaces the diffusion constant D in the expression on the vertical axis.
 - ¹³ I. M. Miron *et al.*, Nature Mater. **9**, 230 (2010).
 - ¹⁴ U. H. Pi *et al.*, Appl. Phys. Lett. **97**, 162507 (2010).
 - ¹⁵ T. Suzuki *et al.*, Appl. Phys. Lett. **98**, 142505 (2011).
 - ¹⁶ A. Chernyshov *et al.*, Nature Physics **5**, 656 (2009).
 - ¹⁷ D. Fang *et al.*, Nature Nanotech. **6**, 413 (2011).
 - ¹⁸ M. Endo, F. Matsukura, and H. Ohno, Appl. Phys. Lett. **97**, 222501 (2010).
 - ¹⁹ I. M. Miron *et al.*, Nature (London) **476**, 189 (2011).
 - ²⁰ K. Obata, and G. Tatara, Phys. Rev. B **77**, 214429 (2008).
 - ²¹ I. M. Miron *et al.*, Nature Mater. **10**, 419 (2011).
 - ²² L. Liu, T. Moriyama, D. C. Ralph, and R. A. Buhrman, Phys. Rev. Lett. **106**, 036601 (2011); Science **336**, 555 (2012).
 - ²³ A. Manchon, arXiv:1204.4869.
 - ²⁴ J. Rammer and H. Smith, Rev. Mod. Phys. **58**, 323 (1986).
 - ²⁵ E. G. Mishchenko, A. V. Shytov, and B. I. Halperin, Phys. Rev. Lett. **93**, 226602 (2004).
 - ²⁶ J. Rammer, *Quantum Field Theory of Non-equilibrium States* (Cambridge University Press, Cambridge, 2007).
 - ²⁷ S. Zhang and Z. Li, Phys. Rev. Lett. **93**, 127204 (2004).
 - ²⁸ S. Zhang, P. M. Levy, and A. Fert, Phys. Rev. Lett. **88**, 236601 (2002).
 - ²⁹ Y. Tserkovnyak, A. Brataas, G. E. W. Bauer, and B. I. Halperin, Rev. Mod. Phys. **77**, 1375 (2005).
 - ³⁰ Y. Tserkovnyak, E. M. Hankiewicz, and G. Vignale, Phys. Rev. B **79**, 094415 (2009).
 - ³¹ A. A. Burkov, A. V. Núñez, and A. H. MacDonald, Phys. Rev. B **70**, 155308 (2004).
 - ³² İ. Adagideli and G. E. W. Bauer, Phys. Rev. Lett. **95**, 256602 (2005).
 - ³³ R. Winkler, *Spin-Orbit Coupling Effects in Two-Dimensional Electron and Hole Systems*, Springer, Berlin, (2003).
 - ³⁴ S. LaShell, B. A. McDougall, and E. Jensen, Phys. Rev. Lett. **77**, 3419 (1996); F. Reinert *et al.*, Phys. Rev. B **63**, 115415 (2001); G. Nicolay, F. Reinert, S. Hfner, and P. Blaha, Phys. Rev. B **65**, 033407 (2001); M. Hoesch *et al.*, Phys. Rev. B **69**, 241401(R) (2004).
 - ³⁵ O. Krupin *et al.*, Phys. Rev. B **71**, 201403(R) (2005); O. Krupin *et al.*, New. J. Phys. **11**, 013035 (2009).
 - ³⁶ Ph. Hofmann, Prog. Surf. Sci. **81**, 191 (2006); T. Hirahara *et al.*, Phys. Rev. B **76**, 153305 (2007); H. Mirhosseini *et al.*, Phys. Rev. B **79**, 245428 (2009); A. Takayama, T. Sato, S. Souma, and T. Takahashi, Phys. Rev. Lett. **106**, 166401 (2011); K. Ishizaka *et al.*, Nature Mater. **10**, 521 (2011).
 - ³⁷ A. Varykhalov *et al.*, Phys. Rev. Lett. **101**, 256601 (2008); J. Hugo Dil *et al.*, Phys. Rev. Lett. **101**, 266802 (2008); A. G. Rybkin *et al.*, Phys. Rev. B **82**, 233403 (2010).
 - ³⁸ A. D. Caviglia *et al.*, Phys. Rev. Lett. **104**, 126803 (2010).
 - ³⁹ A. N. Chantis, K. D. Belashchenko, E. Y. Tsymbal, and M. van Schilfgaarde, Phys. Rev. Lett. **98**, 046601 (2007).
 - ⁴⁰ G. Bihlmayer, S. Blügel, and E. V. Chulkov, Phys. Rev. B **75**, 195414 (2007); G. Bihlmayer *et al.*, Surf. Sci. **600**, 3888 (2006); M. Nagano *et al.*, J. Phys.: Cond. Mater. **21**, 064239 (2009).
 - ⁴¹ L. Petersen and P. Hedegård, Surf. Sci. **459**, 49 (2000).
 - ⁴² S. R. Park *et al.*, Phys. Rev. Lett. **107**, 156803 (2011).
 - ⁴³ K. Kyuno, R. Yamamoto, and S. Asano, J. Phys. Soc. Jpn. **61**, 2099 (1992); D. Weller *et al.*, Phys. Rev. B **49**, 12888 (1994); G. H. O. Daalderop, P. J. Kelly, and M. F. H. Schuurmans, Phys. Rev. B **50**, 9989 (1994).
 - ⁴⁴ H. X. Yang *et al.*, Phys. Rev. B **84**, 054401 (2011); C. Nistor *et al.*, Phys. Rev. B **84**, 054464 (2011).
 - ⁴⁵ J. Moser *et al.*, Phys. Rev. Lett., **99**, 056601 (2007); A. Matos-Abiad and J. Fabian, Phys. Rev. B, **79**, 155303, (2009).
 - ⁴⁶ A. Manchon, Phys. Rev. B **83**, 172403 (2011); IEEE Trans. Magn. **47**, 2735 (2011); L. Xu and S. Zhang, J. Appl. Phys. **111**, 07C501 (2012).
 - ⁴⁷ S. Smirnov, Phys. Rev. B **83**, 081308(R) (2011).

- ⁴⁸ J. E. Hirsch, Phys. Rev. Lett. **83**, 1834 (1999); S. Zhang, Phys. Rev. Lett. **85**, 393 (2000).
- ⁴⁹ S. Takahashi and S. Maekawa, J. Phys. Soc. Jpn. **77**, 031009 (2008).
- ⁵⁰ A. Vedyayev *et al.*, arXiv:1108.2589 (2011).
- ⁵¹ S. Wang, Yuan Xu, and Ke Xia, Phys. Rev. B **77**, 184430 (2008).
- ⁵² K. W. Kim, S.-M. Seo, J. Ryu, K.-J. Lee, and H.-W. Lee arXiv:1111.3422; S.-M. Seo, K.-W. Kim, J. Ryu, H.-W. Lee, and K.-J. Lee, arXiv:1202.3450.